J|A|C|S
ARTICLES
Published on Web 01/01/2003

Ion Atmosphere Relaxation Control of Electron Transfer Dynamics in a Plasticized Carbon Dioxide Redox Polyether Melt

Dongil Lee, Amanda S. Harper, Joseph M. DeSimone,* and Royce W. Murray*

Contribution from the Kenan Laboratories of Chemistry and NSF Science & Technology Center for Environmentally Responsible Solvents and Processes, University of North Carolina, Chapel Hill, North Carolina 27599

Received September 26, 2002; E-mail: rwm@email.unc.edu

Abstract: The sorption of CO_2 into the highly viscous, semisolid hybrid redox polyether melt, [Co(phenanthroline)$_3$](MePEG-SO$_3$)$_2$, where MePEG-SO$_3$ is a MW 350 polyether-tailed sulfonate anion, remarkably accelerates charge transport in this molten salt material. Electrochemical measurements show that as CO_2 pressure is increased from 0 to 800 psi (54 atm) at 23 °C, the physical diffusion coefficient D_{PHYS} of the Co(II) species, the rate constant k_{EX} for Co(II/I) electron self-exchange, and the physical diffusion coefficient of the counterion $D_{COUNTERION}$ all increase, from 4.3×10^{-10} to 6.4×10^{-9} cm^2/s, 4.1×10^6 to 1.6×10^7 M^{-1} s^{-1}, and 3.3×10^{-9} to 1.6×10^{-8} cm^2/s, respectively. Plots of log(k_{EX}) versus log(D_{PHYS}) and of log(k_{EX}) versus log($D_{COUNTERION}$) are linear, showing that electron self-exchange rate constants are closely associated with processes that also govern D_{PHYS} and $D_{COUNTERION}$. Slopes of the plots are 0.68 and 0.98, respectively, indicating a better linear correlation between k_{EX} and $D_{COUNTERION}$. The evidence indicates that k_{EX} can be controlled by relaxation of the counterion atmosphere about the Co complexes in the semisolid redox polyether melts. Because the counterion relaxation is in turn controlled by polyether "solvent" fluctuations, this is a new form of solvent dynamics control of electron transfer.

Introduction

Electron transfer over nanoscale dimensions in molecular solids and semisolids is a topic that is both fundamentally and technologically significant,[1] yet experimental evidence delineating the factors that control the electron transport dynamics remains incomplete. Our laboratory has probed this topic by combining redox-active moieties with polyether oligomers to produce room-temperature melts[2] that are amorphous, highly viscous, semisolids. These semisolid hybrid redox polyethers (we shall call them simply "redox melts" or "melts") are structurally versatile model media in which to study charge transfer dynamics. The polyether chains serve as a highly viscous, semirigid "solvent" shell, whose properties influence the dynamics of mass, ion, and electron-hopping charge transport. The redox melts are very concentrated so that currents in microelectrode voltammetry of the undiluted melts are substantially controlled by the electron self-exchange reactions (i.e., electron hopping) that occur in the mixed valent diffusion layer created around the working electrode by the electrochemical reaction. The resulting apparent diffusion coefficient (D_{APP}) can be expressed as a summation of a physical diffusion coefficient (D_{PHYS}) with an electron (hopping) diffusion coefficient (D_E), given by the Dahms−Ruff equation:[3]

$$D_{APP} = D_{PHYS} + D_E = D_{PHYS} + \frac{k_{EX}\delta^2 C}{6} \qquad (1)$$

where k_{EX} is the electron self-exchange rate constant of the redox couple of the melt, δ is the equilibrium center-to-center distance between electron donor and acceptor, and C is the total concentration of redox sites in the melts.

Homogeneous electron transfer rate constants (k_{EX}) in hybrid redox polyether melts have been found to be generally smaller, and the (thermal) activation barriers have been found to be larger, than those for analogous reactions in dilute fluid solutions. The experimental barrier energies are also larger than outer-sphere reorganization barrier energies predicted from classical Marcus theory,[4] even for nominally outer-sphere reactions. The molecular reason(s) for these differences are an

(1) (a) Segal, D.; Nitzan, A.; Davis, W. B.; Wasielewski, M. R.; Ratner, M. A. *J. Phys. Chem. B* **2000**, *104*, 3817. (b) Davis, W. B.; Ratner, M. A.; Wasielewski, M. R. *J. Am. Chem. Soc.* **2001**, *123*, 7877. (c) Berlin, Y. A.; Burin, A. L.; Ratner, M. A. *J. Am. Chem. Soc.* **2001**, *123*, 260. (d) Chen, P.; Meyer, T. J. *Chem. Rev.* **1998**, *98*, 1439. (e) Barbara, P. F.; Meyer, T. J.; Ratner, M. A. *J. Phys. Chem.* **1996**, *100*, 13148.

(2) (a) Velazquez, C. S.; Hutchison, J. E.; Murray, R. W. *J. Am. Chem. Soc.* **1993**, *115*, 7896. (b) Poupart, M. W.; Velazquez, C. S.; Hassett, K.; Porat, Z.; Haas, O.; Terrill, R. H.; Murray, R. W. *J. Am. Chem. Soc.* **1994**, *116*, 1165. (c) Long, J. W.; Kim, I. K.; Murray, R. W. *J. Am. Chem. Soc.* **1997**, *119*, 11510. (d) Dickinson, E. V.; Williams, M. E.; Hendrickson, S. M.; Masui, H.; Murray, R. W. *J. Am. Chem. Soc.* **1999**, *121*, 613.

(3) (a) Dahms, H. *J. Phys. Chem.* **1968**, *72*, 362. (b) Ruff, I.; Friedrich, V. *J. Phys. Chem.* **1971**, *75*, 3297. (c) Majda, M. In *Molecular Design of Electrode Surfaces*; Murray, R. W., Ed.; John Wiley & Sons: New York, 1992; pp 159−206.

(4) (a) Marcus, R. A.; Sutin, N. *Biochim. Biophys. Acta* **1985**, *811*, 265. (b) Marcus, R. A.; Siddarth, P. In *Photoprocesses in Transition Metal Complexes, Biosystems, and Other Molecules*; Kochanski, E., Ed.; Kluwer Academic Publishers: Dordrecht, The Netherlands, 1992. (c) Sutin, N. *Acc. Chem. Res.* **1982**, *15*, 275. (d) Sutin, N. *Prog. Inorg. Chem.* **1983**, *30*, 441. (e) Hush, N. S. *Coord. Chem. Rev.* **1985**, *64*, 135.

10.1021/ja0287128 CCC: $25.00

ongoing part of our investigation and are, at least in part, resolved here. On the basis of a remarkable 10^{11}-fold range of correlation between physical diffusivity (D_{PHYS}) and a Co(III/II) heterogeneous electron transfer rate constant, we have speculated[5] that electron transfer and physical diffusion rates might be co-governed by, respectively, repolarization of the ether dipoles in the polyether "solvent shell" and segmental polyether chain motions. The time constants of these latter processes must surely scale with one another.

This report follows a series[5a−c] of investigations in which we have used electrochemical oxidations and reductions of a $[Co^{II}(bpy)_3]^{2+}$ complex, bearing in some manner polyether tails, to measure D_{PHYS} and D_E, respectively, in the semisolid melt. In a recent report,[6] we demonstrated that CO_2 sorption (at high pressure, from a gas/liquid CO_2 bath) accelerates transport properties of the hybrid redox polyether melt, $[Co(bpy-(CO_2MePEG\text{-}350)_2)_3](ClO_4)_2$. CO_2 sorption and its consequent plasticization of the metal complex increase the rate of physical diffusion of the Co(II) complex in the melt, the rate of electron transfers between Co(II) and (electrogenerated upon reduction) Co(I) states of the complex, and the mobility of the metal complex counterions ($D_{COUNTERION}$) in the melt. Accompanying these effects were decreases in activation barrier energies.

This paper expands on that recent report[6] by exploring the CO_2 pressure and temperature dependencies of transport rates in a different highly viscous, semisolid melt, one based on the cationic complex $[Co(1,10\text{-phenanthroline})_3]^{2+}$ combined with MW 350 polyether-tailed sulfonate counterions. This melt complex is abbreviated $[Co(phen)_3](MePEG\text{-}SO_3)_2$. This more extensive study confirms the possibility suggested by the recent report, namely, a new form of solvent dynamics embodied as counterion atmosphere relaxation dynamics. The important contribution is the strong evidence that the semisolid state electron transfer rates of $Co^{II/I}$, and possibly of other semisolid redox systems, may be controlled by the dynamics of counterion atmosphere relaxation, rather than by the intrinsic electron transfer rate itself.

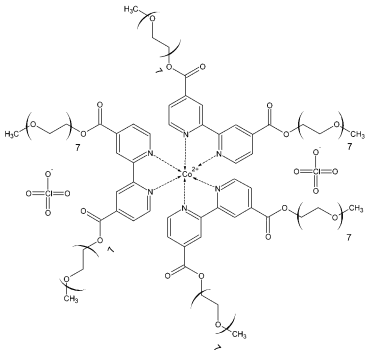

$[Co(bpy(CO_2MePEG\text{-}350)_2)_3](ClO_4)_2$

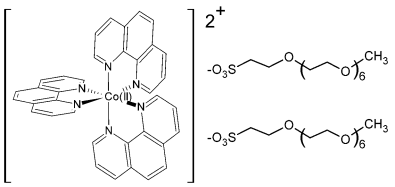

$[Co(phen)_3](MePEG\text{-}SO_3)_2$

Experimental Section

Reagents. SFC/SFE grade of CO_2 (Air Products) was used as received. The polyether-tailed sulfonate counterion ($MePEG\text{-}SO_3^-$)-(H^+) was synthesized as described previously.[7]

Synthesis of $[Co(phen)_3](MePEG\text{-}SO_3)_2$ Melt. Following a previous procedure,[5,7] an aqueous solution of ~700 mg of $MePEG\text{-}SO_3^-Na^+$ was passed through a cation exchange column pretreated with 4 M HCl acid, producing a solution of $MePEG\text{-}SO_3^-H^+$. An aqueous solution of ~500 mg of $[Co(phen)_3](Cl)_2$ was passed through an anion exchange column that had been converted to the OH^- exchange state with 4 M sodium hydroxide. The resulting $[Co(phen)_3](OH)_2$ was immediately titrated to neutrality with the $MePEG\text{-}SO_3^-H^+$ solution, and the water was then removed via vacuum evaporation.

High-Pressure Microelectrode Cell Fabrication. The microelectrode cell used in the pressurized CO_2 bath consists of the tips of four wires exposed in an insulating plane: a small-diameter (25 μm diameter, Goodfellow) Pt wire working electrode, two Pt (0.4 mm diameter) wire electrodes, and a Ag (0.5 mm diameter) wire quasi-reference electrode. The Co complex melt was cast onto this electrode platform and thoroughly dried. In three electrode voltammetry, we make use of one of the two Pt wire counter electrodes. The two 0.4 mm Pt wire (counter) electrodes were used together to measure the ionic conductivities of the melts. The wires were connected to 22-gauge magnet wire (Belden) with silver epoxy (Epo-Tek H2OE, Epoxy Technology Inc.). The group of four electrodes was inserted through a $^1/_4$ in. stainless steel tube and potted in place with an epoxy resin (poly(bisphenol A-*co*-epichlorohydrin), glycidyl end-capped, M_N ca. 377; Aldrich) cross-linked with 14 wt % 1,3-phenylenediamine (Aldrich). Fabrication of the resin with fresh reagents is important to avoid subsequent leaks in contact with CO_2. The end of the assembly was polished with alumina paste (successively smaller grades down to 0.05 μm; Buehler) and cleaned electrochemically in 0.1 M H_2SO_4 solution.[8]

High-Pressure Electrochemical Cell. Electrochemical measurements were performed in a high-pressure cylindrical view cell constructed of 316 stainless steel with a cavity volume of 25 mL. Two sapphire windows (1 in. diameter and $^3/_8$in. thickness, Crystal Systems) were mounted into opposing sides of the cell bottom and held in place with hollow brass bolts and Teflon O-rings. Three $^1/_{16}$ in. Taper Seal ports (High-Pressure Equipment's standard) were machined in the cell for CO_2 inlet/outlet and thermocouple connections. One $^1/_4$ in. NPT port was tapped into the cell for the microelectrode probe. Temperature was controlled within ±0.5 °C of the set temperature using a water jacket connected to a temperature controller (model RTE-110, Neslab). The pressure within the cell was monitored using an output pressure transducer (model TJE AP121DV, Sensotec). High-pressure CO_2 was introduced to the cell using a syringe pump (model 260D, Isco). Safety information regarding handling of high-pressure apparatus is described elsewhere.[9]

High-Pressure Swelling Cell. The extent of CO_2-swelling of the molten salt $[Co(phen)_3](MePEG\text{-}SO_3)_2$ was measured with a high-pressure cell specifically designed to measure volumes at elevated CO_2 pressure.[10] The measured swelling volume and molar volume of the Co complex melt at vacuum (obtained from density measurements) were subsequently used to estimate the concentration of the Co complex

(5) (a) Williams, M. E.; Crooker, J. C.; Pyati, R.; Lyons, L. J.; Murray, R. W. *J. Am. Chem. Soc.* **1997**, *119*, 10249. (b) Williams, M. E.; Masui, H.; Long, J. W.; Malik, J.; Murray, R. W. *J. Am. Chem. Soc.* **1997**, *119*, 1997. (c) Williams, M. E.; Lyons, L. J.; Long, J. W.; Murray, R. W. *J. Phys. Chem. B* **1997**, *101*, 7584. (d) Dickinson, E. V.; Masui, H.; Williams, M. E.; Murray, R. W. *J. Phys. Chem. B* **1999**, *103*, 11028.
(6) Lee, D.; Hutchison, J. C.; Leone, A. M.; DeSimone, J. M.; Murray, R. W. *J. Am. Chem. Soc.* **2002**, *124*, 9310.
(7) Ritchie, J. E.; Murray, R. W. *J. Phys. Chem. B* **2001**, *105*, 11523.
(8) Conway, B. E.; Angerstein-Kozlowska, H.; Sharp, W. B. A.; Criddle, E. E. *Anal. Chem.* **1973**, *45*, 1331.
(9) See, for example: Sullenberger, E. F.; Michael, A. C. *Anal. Chem.* **1993**, *65*, 2304.
(10) Royer, J. R.; DeSimone, J. M.; Khan, S. A. *Macromolecules* **1999**, *32*, 8965.

melt (C), its fractional free volume (FFV),[11] and the equilibrium, center-to-center distance (δ)[12] between Co complexes in the melt at each CO_2 pressure (Supporting Information).

Electrochemical Measurements. Cyclic voltammetry and chronoamperometry of the Co complex redox melt were performed at different CO_2 pressures using a home-built, low-current potentiostat. All measurements were carried out on $[Co(phen)_3](MePEG\text{-}SO_3)_2$ melts to which 3 equiv of MePEG were added to soften the melt and provide ionic conductivity sufficient to support microelectrode voltammetry without CO_2 plasticization. Films of the Co complex melts (ca. 1 mm thick) were cast onto the microelectrode platform and thoroughly dried (sorbed water is a potent plasticizer) under vacuum (ca. 1×10^{-3} Torr) in the high-pressure cell at 70 °C for at least 3 days. Films were equilibrated at each temperature and pressure for at least 2 h prior to measurements. Cyclic voltammograms were used to determine the peak potentials of the Co(II/I) and Co(III/II) waves. For chronoamperometry, potential steps of 400−500 mV starting from a non-Faradaic region and arriving at diffusion-limited potentials of the waves were used. For the Co(III/II) couple, the current decays in a linear diffusion region and was analyzed with the Cottrell equation:

$$I = nFAD^{1/2}C/\pi^{1/2}t^{1/2} \quad (2)$$

where I is current, F is Faraday's constant, A is the microelectrode area, D is the diffusion coefficient, C is concentration (mol/cm^3), and t is time. (The radius of the microelectrode (14.8 μm) was calibrated by voltammetry of ferrocene[13] in acetonitrile.) For the Co(II/I) couple in the melt, the faster, electron-hopping charge transport produces radial diffusion conditions after longer electrolysis time[14] (typically after 2000 s). The resulting steady-state currents (I_{SS}) are analyzed with:[15]

$$I_{SS} = 4nFrDC \quad (3)$$

Ionic conductivities of the melts were measured using a Solartron Model SI 1260 impedance/gain phase analyzer − SI 1287 electrochemical interface combination. Impedance measurements from 1 MHz to 1 Hz were performed at 0 V DC bias and 10−50 mV AC amplitude. (This potential corresponds to ion transport in the melt in the Co(II) state.) Ionic conductivity was calculated as the product of geometric cell constant (22.5 cm^{-1}) and resistance (taken from the low-frequency real-axis intercept of the complex impedance semicircle).

Results and Discussion

Charge Transport in $[Co(phen)_3](MePEG\text{-}SO_3)_2$ at Varied CO_2 Pressures. Figure 1 shows voltammograms of the counterion-tailed cobalt complex melt, $[Co(phen)_3](MePEG\text{-}SO_3)_2$, in baths ranging from vacuum to CO_2 at elevated pressure. Changes in pressure alone have no effect on any of the transport parameters.[16] As observed previously for Co bipyridine complexes,[5,6] the $[Co(II/I)(phen)_3]^{2+}$ reduction current peak at −0.72 V is (at all pressures) much larger than that for the $[Co(III/II)(phen)_3]^{2+}$ oxidation at +0.56 V. This difference in currents occurs, although the same complex, $[Co(phen)_3]^{2+}$, physically diffuses to the electrode in both reactions. The large reduction currents arise from the facile electron self-exchange reactions (hopping) of the Co(II/I) mixed valent diffusion layer in the electrode/melt interfacial region generated by $[Co(phen)_3]^{2+}$ reduction. When the metal complex is oxidized, on the other hand, charge transport by electron hopping in the Co(III/II) diffusion layer is negligible, because of the slow Co(III/II) reaction.[17] The currents measured during Co(III/II) oxidation thus measure solely physical diffusion (D_{PHYS}) of the Co(II) complex, whereas those of the Co(II/I) reduction give an apparent diffusion coefficient comprised of both physical and electron (hopping) diffusion as given in eq 1. The diffusion coefficients for the Co(III/II) (D_{PHYS}) and Co(II/I) reactions ($D_{APP} = D_{PHYS} + D_E$) were determined at 23 °C as a function

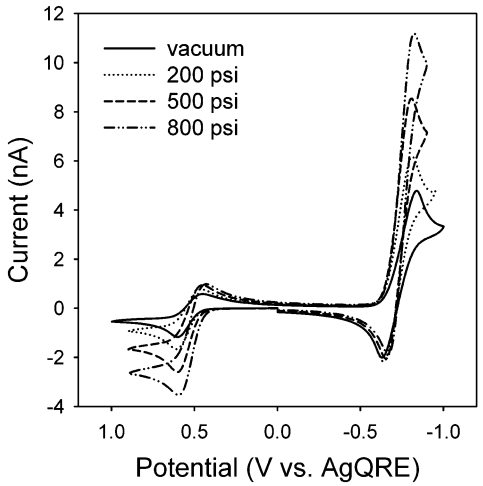

Figure 1. Cyclic voltammograms (5 mV/s) of $[Co(phen)_3](MePEG\text{-}SO_3)_2$ + 3MePEG melt at 14.8 μm radius Pt microdisk electrode at 23 °C and under vacuum or at indicated CO_2 pressures.

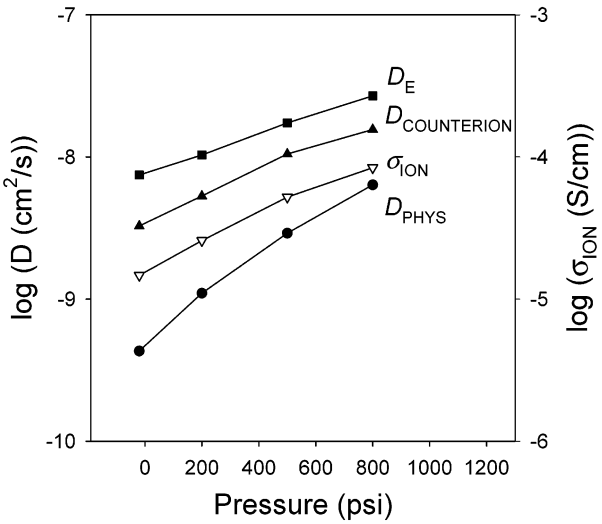

Figure 2. CO_2 pressure dependencies of D_{PHYS}, σ_{ION}, $D_{COUNTERION}$, and D_E in $[Co(phen)_3](MePEG\text{-}SO_3)_2$ + 3MePEG melt at 23 °C.

(11) (a) Fractional free volume (FFV) was estimated from: $FFV = (V_m - V_w)/V_m$, where $V_m = M/\rho$ is the molar volume of the melt, M and ρ are the molecular weight and density of the melt, respectively, and V_w is the estimated van der Waals volume, calculated using a functional group contribution method.[11b−d] (b) Van Krevelen, D. W.; Hoftyzer, P. J. *Properties of Polymers*; Elsevier Scientific Publishing Co.: Amsterdam, 1976. (c) Van Krevelen, D. W.; Hoftyzer, P. J. *J. Appl. Polym. Sci.* **1969**, *13*, 871. (d) Bondi, A. *J. Phys. Chem.* **1964**, *68*, 441.

(12) δ is taken as the equilibrium center-to-center distance between Co complexes and is calculated from the melt density on the basis of a fictitious cubic lattice model. For CO_2-swollen Co complex melt, δ values are estimated from the swollen volume (Supporting Information).

(13) Owlia, A.; Wang, Z.; Rusling, J. F. *J. Am. Chem. Soc.* **1989**, *111*, 5091.

(14) (a) Convection effects on transport are not observed in these viscous media even at a much longer time.[14b] (b) Crooker, J. C.; Murray, R. W. *Anal. Chem.* **2000**, *72*, 3245.

(15) (a) Wightman, R. M. *Anal. Chem.* **1981**, *53*, 1125A. (b) Kovach, P. M.; Lowry, C.; Peters, D. G.; Wightman, R. M. *J. Electroanal. Chem.* **1985**, *185*, 285.

(16) Increasing CO_2 pressure could affect transports in the melt in at least two ways: plasticization of the polymer matrix arising from imbibed CO_2 and compression from the increased hydrostatic pressure. A previous study[6] shows that there is no pressure effect (up to 4000 psi) on D_{PHYS} or D_E in the melts. The observed increases in transport rates are therefore associated with CO_2-swelling and plasticization.

(17) Buttry, D. A.; Anson, F. C. *J. Am. Chem. Soc.* **1983**, *105*, 685.

Table 1. Physical Dynamics and Electron Transfer Results for $[Co(phen)_3](MePEG\text{-}SO_3)_2$ + 3MePEG Melt at a Series of CO_2 Pressures

CO_2 density (g/mL) CO_2 pressure (psi/atm) at 23 °C	0.000 vacuum	0.027 200/13.6	0.078 500/34	0.163 800/54.4
Co concentration (M)[a]	0.47	0.45	0.42	0.39
δ (Å)[a]	15.2	15.4	15.8	16.2
D_{PHYS} (23 °C) Co(III/II) (cm^2/s)[b]	4.3×10^{-10}	1.1×10^{-9}	2.9×10^{-9}	6.4×10^{-9}
$D_{COUNTERION}$ (23 °C) (cm^2/s)[c]	3.3×10^{-9}	5.3×10^{-9}	1.1×10^{-8}	1.6×10^{-8}
D_E (23 °C) Co(II/I) (cm^2/s)[d]	7.5×10^{-9}	1.0×10^{-8}	1.7×10^{-8}	2.7×10^{-8}
$E_{A,PHYS}$ (kJ/mol)[e]	55	44	35	29
$E_{A,ION}$ (kJ/mol)[e]	39	34	27	23
$E_{A,ET}$ (kJ/mol)[e]	36	35	30	27
$t_{COUNTERION}$ (23 °C)[f]	0.79	0.71	0.64	0.55
$D_{COUNTERION}/D_E$	0.44	0.51	0.61	0.58
k_{EX} (23 °C) ($M^{-1}\ s^{-1}$)[g]	4.1×10^6	5.8×10^6	9.9×10^6	1.6×10^7
$K_P\kappa\nu_N$ (23 °C) ($M^{-1}\ s^{-1}$)[h]	9.5×10^{12}	7.6×10^{12}	2.1×10^{12}	8.5×10^{11}
$\exp(-\Delta G^*/RT)$ (23 °C)[i]	4.4×10^{-7}	6.7×10^{-7}	5.1×10^{-6}	1.7×10^{-5}

[a] Estimate from density and swelling volume measurements (Table S1). [b] From Cottrell slope (eq 2) chronoamperometry. [c] Calculated via eq 4. [d] Calculated from eqs 1 and 3. [e] From slopes of activation plots in Figure 4. [f] Transference number for the counterion. [g] Calculated via eq 1. [h] Intercepts of Figure 4 activation plots of k_{EX}. [i] Calculated by using $E_{A,ET}$ values for ΔG^*.

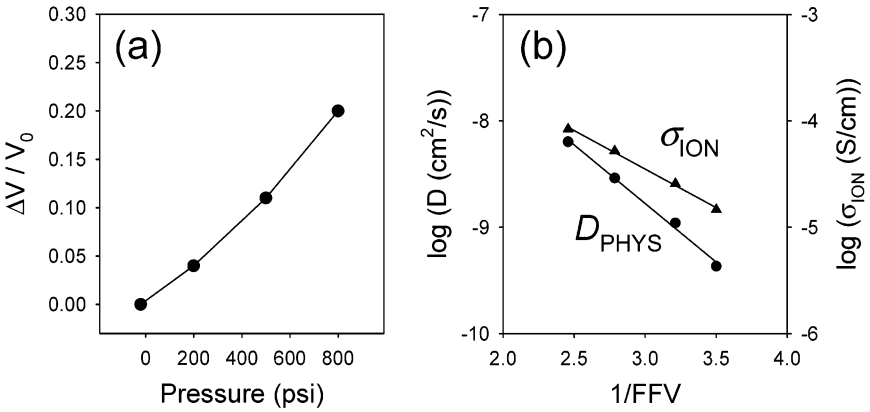

Figure 3. (a) CO_2 pressure dependence of the swelling volume (ΔV) at 23 °C relative to the initial volume (V_0) and (b) relationship between physical diffusivity(D_{PHYS})/ionic conductivity (σ_{ION}) and the reciprocal fractional free volume (1/*FFV*) for CO_2-swollen $[Co(phen)_3](MePEG\text{-}SO_3)_2$ + 3MePEG melt at 23 °C.

of CO_2 pressure with potential step chronoamperometry; the results are presented in Figure 2 and Table 1. Both D_{PHYS} and D_E are remarkably dependent on CO_2 pressure, increasing from vacuum to 800 psi (54 atm) CO_2 by ca. 15-fold and 4-fold, respectively. (The experiments were not carried to higher CO_2 pressures because the MePEG added to the redox melt (see Experimental Section) tended to dissolve at the higher CO_2 densities.) Concurrently, the ionic conductivity σ_{ION} and the $D_{COUNTERION}$ of the Co complex melt also increased (Figure 2 and Table 1) with increasing CO_2 pressure. Observation of a CO_2-induced plasticization effect[6] on D_{PHYS} and $D_{COUNTERION}$ in $[Co(bpy(CO_2MePEG\text{-}350)_2)_3](ClO_4)_2$ melts was noted above; the present data further reflect the close association of polyether chain segmental motions with both Co complex and counterion transport.

It is necessary to detail various corrections to the experimental transport parameters, considering first the concentration dilution of the melt by imbibed CO_2. Figure 3a shows optical swelling volume measurements; the volume of the Co complex melt increases by ca. 20% as CO_2 pressure increases from vacuum to 800 psi (54 atm). Swelling volume-corrected concentrations were used to calculate average Co complex center-to-center distances (δ, given in Table 1) and fractional free volume (*FFV*)[12,18] for each CO_2-swollen melt, as done before.[6] Figure 3b shows that $\log(D_{PHYS})$ and $\log(\sigma_{ION})$ vary linearly with the reciprocal free volume (1/*FFV*), with negative slopes. These observations are consistent with CO_2 being an effective plasticizer of the Co complex melt, by changing its free volume content.

Additional possible corrections involve effects of (a) electronic and (b) ionic migration on the transport results of Table 1. Electronic migration refers to an alteration of the electron-hopping rate (e.g., for Co(II/I)) by electric field gradients in the sample; such gradients typically arise from a small $D_{COUNTERION}$ relative to D_E and can lead to overestimation of D_E.[20] As before,[5b,c,6] $D_{COUNTERION}$ is estimated from the measured ionic conductivities (σ_{ION}) and D_{PHYS} with[19]

$$\sigma_{ION} = \frac{F^2}{RT}[z_{Co}^2 D_{Co} C_{Co} + z_{COUNTERION}^2 D_{COUNTERION} C_{COUNTERION}] \quad (4)$$

where z, D, and C are the charge, diffusion coefficient, and concentration of the indicated species, respectively. The evaluated $D_{COUNTERION}$ values (Table 1) were applied to the migration theory of Saveant.[20] The ratio $D_{COUNTERION}/D_E$ was less than

(18) (a) Flory, P. J. *J. Chem. Phys.* **1950**, *18*, 108. (b) Cohen, M. H.; Turnbull, D. *J. Chem. Phys.* **1959**, *31*, 1164. (c) Stern, S. A.; Saxena, V. *J. Membr. Sci.* **1980**, *7*, 47. (d) Stern, S. A.; Frisch, H. L. *Annu. Rev. Mater. Sci.* **1981**, *11*, 523.
(19) MacCallum, J. R.; Vincent, C. A. *Polymer Electrolyte Reviews*; Elsevier Applied Science: Oxford, U.K., 1987; Vol. 1.
(20) Andrieux, C. P.; Saveant, J. M. *J. Phys. Chem.* **1988**, *92*, 6761.

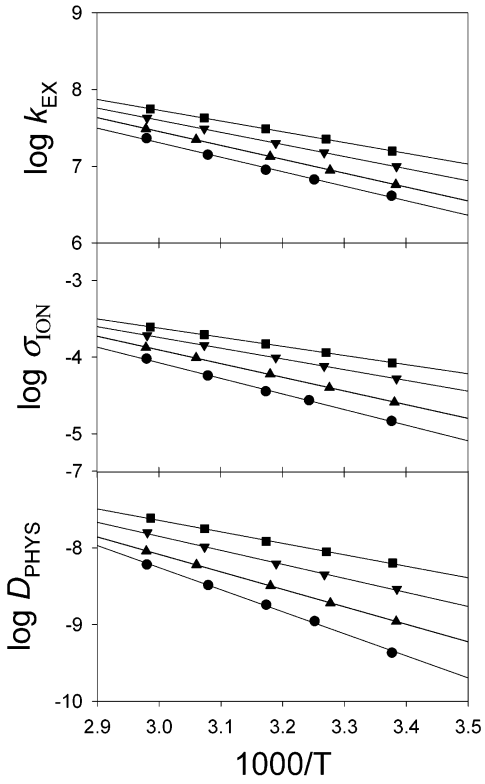

Figure 4. Activation plots of k_{EX} (upper), σ_{ION} (middle), and D_{PHYS} (lower) at varied CO_2 pressures: vacuum (●), 200 (▲), 500 (▼), and 800 psi (■).

one, but only modestly so, and the corrected values of D_E increased by only 10%. The activation parameters ($E_{A,ET}$) obtained from the corrected D_E were unchanged. Ionic migration refers to physical mass transport of an ionic reactant that is aided or retarded by it, supporting a significant portion of the ion flow that accompanies electrode reactions. Ionic migration of a reactant is negligible when the transference number of the other ions (i.e., $t_{COUNTERION}$)[21] is large. Table 1 shows that $t_{COUNTERION}$ is only modestly less than unity, so underestimation of D_{PHYS} because of ionic migration of the Co(II) complex is not significant (worst case ca. 20%). We conclude that migration effects are unimportant in these measurements.

Temperature Effects. Figure 4 shows how D_{PHYS}, σ_{ION}, and the electron self-exchange rate constant k_{EX} (calculated from D_E) change with temperature, and Table 1 gives the associated activation barrier energies $E_{A,PHYS}$, $E_{A,ION}$, and $E_{A,ET}$. The activation barrier energy for D_{PHYS} in a vacuum exceeds those for $D_{COUNTERION}$ and D_E, but all of the barrier energies decline with increasing CO_2 pressure and converge to very similar values at 800 psi (54 atm). The activation barrier energies for $D_{COUNTERION}$ and D_E are similar at all pressures, suggesting that the processes of counterion and electron hopping are closely associated.

The enthalpic activation barrier energy for the Co(II/I) electron transfer reaction can be equated with the activation free energy because the self-exchange reaction is symmetrical (in which case[4b,22] reaction entropy and activation entropy are zero).

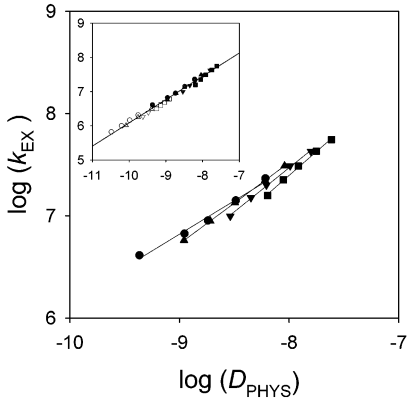

Figure 5. Relationship between k_{EX} for Co(II/I) reaction and D_{PHYS} for Co(III/II) reaction measured at various temperatures (23−62 °C) in $[Co(phen)_3](MePEG\text{-}SO_3)_2$ + 3MePEG melt at varied CO_2 pressures: vacuum (●), 200 (▲), 500 (▼), and 800 psi (■). Slopes are 0.65, 0.79, 0.86, and 0.94 at vacuum, 200, 500, and 800 psi, respectively. Inset: k_{EX} vs D_{PHYS} in $[Co(phen)_3](MePEG\text{-}SO_3)_2$ + 3MePEG melt (filled symbols) and $[Co(bpy(CO_2MePEG\text{-}350)_2)_3](ClO_4)_2$ melt (open symbols, reproduced from ref 6).

Thus, the temperature dependence of the electron transfer reaction rate constant can be expressed by[4]

$$k_{EX} = K_P \kappa \nu_N \exp\left[-\frac{\Delta G^*}{RT}\right] \qquad (5)$$

where the experimental activation enthalpy $E_{A,ET} \approx \Delta G^*$ ($=\lambda/4$, where λ is the reorganizational energy, and the reaction free energy is small[4,22]), K_P is the donor−acceptor precursor complex formation constant, κ is the electronic transmission coefficient, and ν_N is the nuclear frequency factor.

CO_2-swelling-induced changes in the rate constant k_{EX} can, according to eq 5, arise from changes either in $E_{A,ET}$ or in the preexponential term. The decrease in $E_{A,ET}$ from 36 to 27 kJ/mol (from vacuum to 800 psi, Table 1) should produce an ca. 40-fold increase in k_{EX}, but only a 4-fold change is actually seen. Table 1 shows that a contravening ca. 10-fold decrease in the preexponential term ($K_P\kappa\nu_N$) occurs with increasing CO_2 pressure (although the relatively small temperature interval and long extrapolation of the Figure 4 activation plots entail a considerable uncertainty). The precursor complex formation constant K_P is near unity[5b] and is unlikely to exhibit a large pressure-dependency, so the preexponential changes are associated with $\kappa\nu_N$. While the change in $\kappa\nu_N$ is in the direction of the electron transfer reaction becoming less adiabatic with increasing CO_2 pressure, all of the $\kappa\nu_N$ values are quite large and consistent with overall adiabatic behavior. The ca. 1 Å change in the average metal complex spacing in the melt (δ in Table 1) is not believed to be large enough to weaken the electronic coupling between the Co complex reactants. By elimination, we point then to changes in the nuclear factor ν_N as the likely source of increase in k_{EX} with increasing CO_2 plasticization. Recent measurements[23] of the rate of the heterogeneous Co(III/II) electron transfer reaction in this melt when the added plasticizer is MePEG lead to a similar conclusion.

Electron Transfer-Diffusivity Correlation. Figure 5 shows log−log plots of the Table 1 k_{EX} and D_{PHYS} results. The four lines in Figure 5 are for different pressures; the variations in

(21) Bard, A. J.; Faulkner, L. R. *Electrochemical Methods: Fundamentals and Applications*, 2nd ed.; John Wiley & Sons: New York, 2001; p 67.
(22) (a) Newton, M. D.; Sutin, N. *Annu. Rev. Phys. Chem.* **1984**, *35*, 437. (b) Sutin, N.; Brunschwig, B. S.; Creutz, C.; Winkler, J. R. *Pure Appl. Chem.* **1988**, *60*, 1817.
(23) Harper, A. S.; Lee, D.; Murray, R. W., manuscript in preparation.

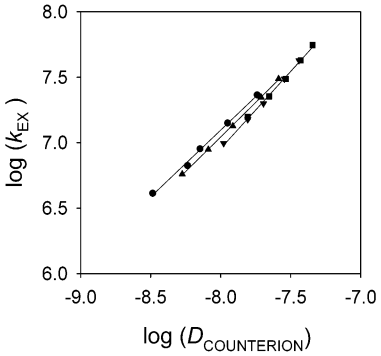

Figure 6. Relationship between k_{EX} for Co(II/I) reaction and $D_{COUNTERION}$ measured at various temperatures (23−62 °C) in $[Co(phen)_3](MePEG\text{-}SO_3)_2$ + 3MePEG melt at varied CO_2 pressures: vacuum (●), 200 (▲), 500 (▼), and 800 psi (■). Slopes are 1.02, 1.06, 1.18, and 1.18 at vacuum, 200, 500, and 800 psi, respectively.

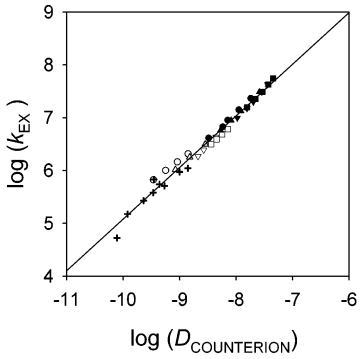

Figure 7. k_{EX} vs $D_{COUNTERION}$ for $[Co(phen)_3](MePEG\text{-}SO_3)_2$ + 3MePEG melt (filled symbols), $[Co(bpy(CO_2MePEG\text{-}350)_2)_3](ClO_4)_2$ melt (open symbols, from ref 6), and $[Co(bpy(CO_2MePEG\text{-}350)_2)_3](ClO_4)_2 + xLiClO_4$ melt (crosses, $x = 0-1.31$, from ref 5c).

k_{EX} and D_{PHYS} on each line are produced by temperature variation. The slopes of the four linear plots range from 0.65 to 0.94; the largest slope occurs at the highest pressure (highest degree of CO_2 plasticization). The Figure 5 inset shows a plot combining the present $[Co(phen)_3](MePEG\text{-}SO_3)_2$ with previous[6] $[Co(bpy(CO_2MePEG\text{-}350)_2)_3](ClO_4)_2$ melt data for all temperatures and pressures. The striking near-linear correlation has a slope of 0.68 and extends over a range of roughly 10^3-fold in D_{PHYS}.

An even better correlation between physical diffusivity and electron transfer rates is obtained if one represents physical diffusivity with $D_{COUNTERION}$ rather than with D_{PHYS}. The diffusion coefficients of the melt counterion (polyether-tailed sulfonate in the present case, perchlorate in the other Co complex melt[6]) are obtained from ionic conductivity data and eq 4 as described above. The actual values of $D_{COUNTERION}$ (Table 1) are strikingly similar to the D_E results and vary with CO_2 pressure in a similar manner, and their activation barrier energies are nearly identical. This correspondence is displayed in log−log plots of D_E and $D_{COUNTERION}$ in Figure 6, where the four lines again represent temperature dependencies at constant pressure. The slopes of the lines in Figure 6 range from 1.0 to 1.2. The correlation between Co(II/I) electron transfer rate constant k_{EX} and $D_{COUNTERION}$ is seen to be excellent in the $[Co(phen)_3](MePEG\text{-}SO_3)_2$ melt.

Figure 7 expands the comparison between k_{EX} and $D_{COUNTERION}$ by adding to the Figure 6 data (filled symbols), previous results in which the counterion was perchlorate. These previous data are for the $[Co(bpy(CO_2MePEG\text{-}350)_2)_3](ClO_4)_2$ (open symbols) melt, where rate variations were provoked in one study by changes in CO_2 pressure and temperature[6] and in another by the dissolution of various amounts of $LiClO_4$ electrolyte in the $[Co(bpy(CO_2MePEG\text{-}350)_2)_3](ClO_4)_2$ (under vacuum at room temperature).[5c] (In the latter case, rate variations are not plasticization, but are associated with chain cross-linking by Li^+ cation/polyether coordination, resulting in a decrease in chain segmental mobility in the melt.) The correlation among the collected data in Figure 7 is excellent, with a slope of 0.98 (i.e., essentially unity), extending over a 10^3-fold range of values. That the slope is nearer to unity than in the Figure 5 inset implies that the dynamics of polyether environment fluctuations that support a diffusive mass transport hop of a *small* entity (perchlorate or the sulfonate headgroups of the polyether chain) are more closely representative of events controlling electron transfer rates than are the polyether fluctuations supporting diffusive transport of a *large* entity (the Co complex).

Consideration of Electron Transfer Dynamics. A related redox melt containing Co bipyridine complexes ($[Co(bpy\text{-}(CO_2MePEG\text{-}350)_2)_3](ClO_4)_2$) displayed[6] a strong correlation between changes in Co(II/I) electron transfer and Co(II) complex physical diffusion rates induced by CO_2-swelling-plasticization. This and other diffusion rate-electron transfer rate correlations[5a,24] have been interpreted in terms of so-called "solvent dynamics" control of the electron transfer rate. In the redox melts,[5,6] the "solvent" can be considered as the polyether chains (the source of free volume for physical transport motions as represented in Figure 3 and previously[5d]). The suggestion is that the rate of dipolar reorganization of the ether dipoles and concurrent chain segmental motions in the polyether chain assume synonymous rate control of electron transfer and physical transport, respectively.

Next we briefly trace a theoretical rationale for a connection between electron transfer rates and physical diffusivity. For electron transfer reactions under adiabatic solvent dynamics control, solvent dipolar fluctuations influence ν_N through the barrier crossing frequency, provided the solvent fluctuations and the transition-state motion are closely coupled:[25]

$$\nu_N = \tau_L^{-1}\left[\frac{\Delta G^*_{OS}}{4\pi RT}\right]^{1/2} \qquad (6)$$

where ΔG^*_{OS} is the outer-sphere reorganizational barrier energy, and τ_L is the longitudinal solvent relaxation time or time constant for solvent dipole reorganization. As noted above, while the melts are highly concentrated in ions, they also contain a significant amount[5d] of polyether "solvent." The reorganization in the bath surrounding the donor−acceptor pairs is comprised of both polyether and ion dipole fluctuations, making the overall process more complicated, with no available explicit τ_L values. Nonetheless, eq 6 is a useful theoretical framework, within

(24) (a) Zhang, X.; Leddy, J.; Bard, A. J. *J. Am. Chem. Soc.* **1985**, *107*, 3719. (b) Zhang, X.; Yang, H.; Bard, A. J. *J. Am. Chem. Soc.* **1987**, *109*, 1916. (c) Miao, W.; Ding, Z.; Bard, A. J. *J. Phys. Chem. B* **2002**, *106*, 1392. (d) Gu, N.; Zhou, H.; Ding, L.; Shi, Z.; Dong, S. *Solid State Ionics* **2000**, *138*, 123. (e) Zhou, H.; Dong, S. *J. Electroanal. Chem.* **1997**, *425*, 55. (f) Pyati, R.; Murray, R. W. *J. Am. Chem. Soc.* **1996**, *118*, 1743.

(25) (a) Weaver, M. J. *Chem. Rev.* **1992**, *92*, 463. (b) Fawcett, W. R.; Opallo, M. *Angew. Chem., Int. Ed. Engl.* **1994**, *33*, 2131. (c) Zusman, L. D. *Chem. Phys.* **1980**, *49*, 295. (d) Calef, D. F.; Wolynes, P. G. *J. Phys. Chem.* **1983**, *87*, 3387. (e) Heitele, H. *Angew. Chem., Int. Ed. Engl.* **1993**, *32*, 359.

which τ_L can be further related[25] to diffusion coefficients (D) by the Debye[24b,26] and Stokes−Einstein equations[24b]

$$\tau_L^{-1} = \frac{\epsilon_S}{\epsilon_{OP}\tau_D} = \left(\frac{\epsilon_S}{\epsilon_{OP}}\right)\frac{3r_H D}{2\alpha^3} \quad (7)$$

where ϵ_{op} and ϵ_s are the optical and static dielectric constants, respectively, τ_D is the Debye relaxation time, α is the molecular radius, and r_H is the hydrodynamic radius. This prediction of an inverse relation between τ_L and D is taken, for the present purposes, as an inverse relation between the rate of effective dipolar reorganization in the melt and the rate of physical diffusion of an object in it, with probably some difference in the proportionality constant connecting the two.

The combination of eqs 6 and 7 forms the basis for expecting correlations between physical diffusivity and electron transfer rate, by way of the effective solvent dipolar relaxation (τ_L), as used previously[24] and as examined in Figures 5 and 7. In Figure 5, the correlation relies on measuring physical diffusivity with D_{PHYS} and is good but nonetheless is not exactly linear (i.e., the log−log slope is less than unity). It has been seen previously[25b,27] that electron transfer rates can vary with $\tau_L{}^{-\theta}$ ($0 < \theta < 1$) when the reaction adiabaticity is weak or inner-sphere reorganizational energy is large, weakening the dependence of the preexponential factor on solvent. We suppose that the $\theta < 1$ in Figure 5 must reflect weakness in the coupling between a Co(II/I) electron transfer and a Co(II) diffusive hop; the polyether environment fluctuations that lead to dipole reorganization for the electron hop are not exactly the same as those that take place in the course of a diffusive mass transport hop. That there is some coupling, however, is clear from the results in Figure 5 and in preceding papers.[5a,6]

An alternative analysis uses the counterion physical diffusivity as a measure of solvent dipolar relaxation and thus of k_{EX}. This model of solvent dynamics control of the electron transfer rate is parallel to that discussed for Figure 5, but Figures 6 and 7 show that $D_{COUNTERION}$ seems to be a superior measure of τ_L.

However, there is *another* way to interpret Figures 6 and 7, in terms of $D_{COUNTERION}$, that has more profound implications for the meaning of experimental values of k_{EX}. We refer to predictions of Figures 6 and 7 behavior derived from theory written[28] for ion pairing effects on electron transfer reactions. The redox ions and counterions in the melts can be considered to be intrinsically ion paired (at least of the solvent separated kind). The relocation of cationic charge that accompanies a Co(II/I) electron transfer must be accompanied not only by the usual reorganization of solvent dipoles, but also, in addition, by a redistribution of the counterions, that is, *relaxation of the ionic atmosphere around the Co(II/I) reaction pair*. The most general case of such relaxation corresponds to "ion transfer accompanying the electron transfer" (case III).[28] For simplicity, we consider a limiting case (case I),[28] in which electron transfer occurs at some counterion position followed by ionic atmosphere relaxation. The reaction is thereby cast as a two-step process:

$$X^-Co^{II}Co^I \underset{k_{-1}}{\overset{k_1}{\rightleftarrows}} X^-Co^ICo^{II} \xrightarrow{k_2} Co^ICo^{II}X^- \quad (8)$$

in which the electron transfer rate constant is given by

$$\frac{1}{k_{EX}} = \frac{1}{k_1} + \frac{k_{-1}}{k_2 k_1} \quad (9)$$

and the counterion relaxation rate constant (k_2) can be represented as a diffusive motion (D, also given by the classical Einstein equation[29]) given by[28]

$$k_2 = D\left(\frac{\pi}{2a}\right)^2 \quad (10)$$

where a is the counterion diffusion length or (case III) the overall rate constant for diffusive steps before and after the electron transfer reaction. Considering eq 9, we find that, if its right-hand term is dominant, *the experimental electron transfer rate constant k_{EX} becomes proportional to, and controlled by, the counterion diffusivity $D_{COUNTERION}$*, just as is observed in Figures 6 and 7.

We briefly examined the above scenario of counterion atmosphere relaxation (or reorganization) in a recent study.[6] The new data convey a broader and more conclusive case, based on two different melt systems containing two different counterions and two different plasticizers, that ionic atmosphere relaxation could provide a connection between physical diffusion and electron transfer rates. The connection differs from "solvent dynamics" in its usual context of solvent dipolar relaxation, in that the rate of counterion atmosphere relaxation, as expressed in eqs 9 and 10 above, is the signal factor controlling k_{EX}. This is then a kind of "solvent dynamics" in which the solvent dipolar fluctuations (and PEG chain segmental motions) govern $D_{COUNTERION}$, and it in turn controls the overall rate of electron transfer. In the context of eq 9, the counterion atmosphere relaxation rate is decoupled from what would be considered classical solvent dipolar relaxation "solvent dynamics" control of k_{EX}. The crucial facet of this new interpretation is that the *overall rate of the electron transfer is not the intrinsic rate, but the diffusion rate of the counterion.*

Coupling between counterion diffusivity and electron transfer rates has been discussed[3c,20,30] before in the contexts of charge compensation and electronic migration effects. The present study reveals that the counterion diffusion and the electron transfer can be strongly coupled in highly viscous redox polymers and semisolids even when the counterion transport is sufficiently fast that these other factors are not significant. In addition, in another study[31] from this laboratory, we have shown by finding percolative behavior that when the redox counterion diffusivity is negligible (i.e., the counterion is a polymer like DNA or sulfonated polystyrene), its sites are Co(II/I) electron transfer inactive despite the presence of other Co(II) complex sites that have diffusive perchlorate counterions and are electron transfer active. Finally, we have puzzled[5b,d,32] why the activation barrier

(26) (a) Hasted, J. B. *Aqueous Dielectrics*; Chapman and Hall: London, 1973. (b) Smyth, C. P. *Dielectric Behavior and Structure*; McGraw-Hill: New York, 1955.
(27) (a) Fawcett, W. R.; Opallo, M. *J. Phys. Chem.* **1992**, *96*, 2920. (b) Fawcett, W. R.; Opallo, M. *J. Electroanal. Chem.* **1993**, *349*, 273. (c) Fawcett, W. R.; Opallo, M. *J. Electroanal. Chem.* **1992**, *331*, 815.
(28) Marcus, R. A. *J. Phys. Chem. B* **1998**, *102*, 10071.
(29) Bard, A. J.; Faulkner, L. R. *Electrochemical Methods: Fundamentals and Applications*, 2nd ed.; John Wiley & Sons: New York, 2001; p 147.
(30) (a) Majda, M.; Faulkner, L. R. *J. Electroanal. Chem.* **1982**, *137*, 149. (b) Surridge, N. A.; Sosnoff, C. S.; Schmehl, R.; Facci, J. S.; Murray, R. W. *J. Phys. Chem.* **1994**, *98*, 917. (c) Saveant, J.-M. *J. Electroanal. Chem.* **1988**, *242*, 1.
(31) Leone, A. M.; Tibodeau, J. D.; Thorp, H. H.; Murray, R. W., manuscript in preparation.
(32) Masui, H.; Murray, R. W. *Inorg. Chem.* **1997**, *36*, 5118.

energies for electron transfers are so much larger than the 8−10 kJ/mol energies estimated for an "outer-sphere" reaction form the classical Marcus dielectric continuum model.[4a] Following the eqs 9 and 10 analysis of the data, Table 1 (and the previous study[6]) shows that, while $E_{A,ET}$ is larger than the classical estimate, it is nearly equal, and varies identically with CO_2 plasticization, to the barrier for counterion transport, $E_{A,ION}$. It seems likely that it is the thermal barrier to counterion diffusive motion that is experimentally measured, and not the intrinsic electron transfer barrier energy.

Acknowledgment. This research is supported in part by the STC Program of the National Science Foundation under Agreement No. CHE-9876674, and by the Department of Energy, Division of Basic Sciences.

Supporting Information Available: Data on concentration correction (Table S1), and transport (Table S2) for CO_2-swollen $[Co(phen)_3](MePEG\text{-}SO_3)_2$ melt (PDF). This material is available free of charge via the Internet at http://pubs.acs.org.

JA0287128